MECHANICAL TECHNOLOGY INCORPORATED
968 Albany-Shaker Road
Latham, New York 12110

MTI-67TR30

ANALYSIS, DESIGN, AND PROTOTYPE DEVELOPMENT OF SQUEEZE-FILM BEARINGS FOR AB-5 GYRO. 2#

PHASE IV: SUMMARY REPORT

DEVELOPMENT OF A CONICAL-BEARING, AXIAL EXCURSION PROTOTYPE

by

F. K. Orcutt
C. H. T. Pan

April, 1967

NO. MTI-67TR30

DATE: April, 1967

TECHNICAL REPORT

ANALYSIS, DESIGN, AND PROTOTYPE DEVELOPMENT OF SQUEEZE-FILM BEARINGS FOR AB-5 GYRO

PHASE IV SUMMARY REPORT
DEVELOPMENT OF A CONICAL-BEARING, AXIAL EXCURSION PROTOTYPE

by

F. K. Orcutt and C. H. T. Pan

Author(s) C. H. T. Pan, F. K. Orcutt

Approved

Approved

Prepared under

Contract: NAS8-11678

Prepared for

NATIONAL AERONAUTICS AND SPACE ADMINISTRATION
GEORGE C. MARSHALL SPACE FLIGHT CENTER
HUNTSVILLE, ALABAMA

MTI
MECHANICAL TECHNOLOGY INCORPORATED
MTI

968 ALBANY - SHAKER ROAD — LATHAM, NEW YORK — PHONE 785-0922

TABLE OF CONTENTS

INTRODUCTION

In a squeeze film gas bearing, the bearing surfaces are vibrated relative to one another in the plane normal to the surfaces. If the vibration frequency is high, during each cycle of oscillation gas in the space between the bearing surfaces is alternately compressed and expanded. Because of non-linear effects, the integrated pressure in the bearing film over a full cycle of oscillation is greater than the ambient pressure. For this reason, the squeeze-film bearing is able to sustain a load.

This report describes the work done in Phase IV of contract NAS8-11678 toward development of a preliminary prototype squeeze-film bearing system which would ultimately be suitable for gymbal axis support of and AB5 size gyro.

For a given bearing surface geometry and mean gap between surfaces, the bearing load capacity and stiffness increase with increased vibration amplitude. Or, stated another way, specified bearing load capacity and stiffness can be achieved with a larger mean gap if the vibratory motion amplitude is increased. For this reason, the effort to develop a squeeze-film bearing support has centered on the development of the transducer system which provides the high-frequency vibratory motion of the bearing surfaces.

The body of the report describes the work performed under Tasks 1 through 3 of Modification 7 (Phase IV) of Contract NAS8-11678. The experimental evaluation of the NASA built transducer design with Belleville spring coupling between bearing and driver sections (Task 4) is described in Appendix A.

REVIEW OF PREVIOUS TRANSDUCER DEVELOPMENT

Vibratory motion of the bearing surfaces can be achieved through piezoelectric, magnetostrictive or electro-magnetic drivers. Piezoelectric transducers have been preferred over the others because they offer the best combination of high driving frequencies, large vibratory amplitudes, low power dissipation and low weight. Initially, the approach was to have the piezoelectric body serve as the vibrating bearing element. In this concept, the transducer is a tube of piezoceramic material driven at its hoop mode resonant frequency. The float, representing a gyro, fits inside the piezoceramic tube where it is supported radially by squeeze-film action in the intervening annular clearance. Axial support is obtained from squeeze-film action in the clearance between thrust plates attached to either end of the float and the end surfaces of the tube. The transducer tube and float assembly must be positioned and supported within a stationary housing without restraining or appreciably distorting the vibratory motion. This is done also by squeeze-film bearing support between the tube and a cylindrical bore outer housing and with thrust plates attached to the housing in close proximity to the outer section of the tube ends. The development and experimental performance of this concept are described in References 1 and 2. Bendix Corp., Research Laboratories Division developed and fabricated prototype transducers of this type as a subcontractor to MTI. These prototype float supports were evaluated experimentally and they were successful in effecting squeeze-film support of the float. However, there were several disadvantages of this transducer concept:

(1) Vibratory motion amplitudes were very small (about 10^{-4} inch peak-to-peak per inch of bearing diameter) necessitating very small bearing clearances (on the order of 10^{-4} in/in) and exceedingly precise machining.

(2) The plated surfaces of the piezoceramic tube were subject to material transfer and deterioration due to contact during starts. This could be minimized by protective coatings but these were not completely satisfactory.

(3) The motion of the piezoceramic tube is not uniform, due to end effects, so the bearing surface excursion is not uniform which detracts from performance.

(4) It is very difficult to achieve either equal stiffness or equal load capacity in the radial and axial directions because of limited axial bearing area.

An alternative approach was devised in which the bearings are separate elements attached to the piezoelectric driver through flexures (Refs. 3 and 4). An exploratory transducer of this type with conical bearings confirmed that this approach could yield considerably larger motion amplitudes, due to motion amplification through the flexure. Figure 1 illustrates this experimental transducer assembly. A detailed survey of the motions of the bearing surfaces showed the following:

(1) Mean axial excursion amplitudes of about 250 μ in (half-wave amplitude) were achieved with about 10 volt-amps electrical input.

(2) The bearing cone did not move as a rigid body. In addition to the desired axial excursion, there was a rotation of the cone cross section about the connection to the flexure. The translational and twist components were additive at the small diameter end and subtractive at the large diameter end, resulting in a variation in motion measured normal to the bearing surface of about 2 to 1.

A precision male cone section was fabricated and fitted to one of the vibrating female cone ends in order to evaluate the bearing performance in the axial load direction. The results, which are described in detail in Ref. 5, are summarized below:

(1) Measured load capacity compared reasonably well with that derived from squeeze-film bearing theory for low values of excursion ratio (light loads). The results diverged as the excursion ratio was increased with the calculated load capacity exceeding the measured values by an increasing margin. The discrepency is believed to be a result of non-uniform motion and imperfect mating of the test bearing surfaces, and vibratory response of the supported mass.

(2) Introduction of the male bearing cone caused a reduction in female cone motion amplitude by a factor of about 1.6. This motion attenuation was essentially constant with applied load. It appeared to be caused

by viscous damping of the squeeze film.

(3) There was some difficulty with material transfer from the male aluminum cone surface to the molybdenium female cone surface. Protective surface coatings were helpful in preventing this.

DESIGN OF THE PRECISION SQUEEZE-FILM BEARING FLOAT SUPPORT

As a result of the previous work with experimental squeeze-film bearing supports, it was decided to continue with the concept characterized by separate bearing elements attached to the piezoelectric driver through flexures. The first, conical bearing, experimental transducer of this type had been quite successful and the only major area in which improvement was needed was to achieve more uniform motion of the bearing surfaces. In addition, it was decided that spherical segment bearings offered worthwhile advantages over conical segments because of greatly reduced requirements on machining and assembly tolerances for alignment.

The final transducer design, selected for fabrication and evaluation is shown schematically in Figure 2. The bearing segments are anodized aluminum. They are cap screwed and bonded with epoxy to steel flexure sections. This multi-piece design was used in place of the machined-from-one-piece design used for the conical bearing transducer for several reasons:

(a) To obtain high strength and low internal damping properties for the flexure section.

(b) To obtain the stiffness and resistance to twisting offered by a large bearing element cross-sectional area while keeping the mass attached to the flexure low enough to avoid an excessive reduction in operating frequency.

The flexure is in the form of a washer-shaped section bounded at its ID by the heavy section which bears against the end of the piezoceramic tube, and at its OD by the thin cylindrical section which attaches to the bearing segment. The piezoceramic material is Gulton HDT-31 lead zirconate-lead titanate. The thin cylindrical section was incorporated to provide relief for the bearing segment from the twisting moment resulting from deflection of the flexure. The bearing-flexure ends are attached to the ends of the piezoceramic cylinder by 12 tiebolts

which are torqued uniformly in order to achieve 4000 - 5000 lb compressive preload on the joint. The surfaces of the joint are coated with epoxy just prior to assembly in order to increase the effective contact area and thus stiffen the connection.

A triangular-shaped frame is cemented to the piezoceramic tube at its midplane for the purpose of holding, or mounting the entire assembly. The frame can be seen in the photograph of the assembled unit, Figure 3. The triangular configuration was chosen because it offers little restraint to hoop mode vibratory motions of the piezoceramic tube while still providing rigid radial positioning of the tube axis.

True sphericity and close conformity of the bearing surfaces is achieved by lapping the male and female bearing segments together. Both parts are aluminum and they are lapped first after machining using aluminum oxide lapping compound until at least 95 per cent contact is established. Both parts are then anodized and they are then finish lapped using diamond compound. Thus, the radii of curvature of the bearing parts are identical and the bearing clearance is obtained by introducing axial end shake.

As a result of experimental observations, which will be described, a modification was undertaken for the purpose of obtaining a stiffer, more uniform connection between the flexure and bearing sections. This modification, illustrated by Figure 4, results in a cap-screwed, epoxy-filled joint loaded in direct bearing instead of in shear. The modification required fabrication of new steel flexure sections. The same female bearing sections were modified and used.

TRANSDUCER DESIGN

Design analysis curves for the axial-excursion squeeze-film bearing transducer are given in Ref. 3. The pertinent calculated design parameters for the spherical-bearing transducer designs are given in Table 1:

TABLE I

CALCULATED DESIGN PARAMETERS OF PRECISION SQUEEZE - FILM BEARING TRANSDUCERS

	Original Design	Modified Design
Axial mode resonant frequency of piezoceramic tube, kHz	33	33
Weight of end parts rigidly attached to tube, lb.	.62	.66
Axial mode resonant frequency of driver section including rigidly attached parts, kHz	21.0	20.4
Weight of flexure attached parts, lb.	.68	.797
Ratio of driver section mass to bearing section mass. $\frac{(A_1 \rho_1 \ell)}{m_b}$	2.31	2.02
Flexure stiffness, lb/in x 10^6	5.0	5.0
Ratio of driver section stiffness to flexure stiffness, $\frac{A_1 E_1}{k\ell}$	10	10
Operating Frequency kHz	5.7	5.62
Amplification Factor ($\frac{C_3}{\alpha \epsilon_o}$)	$\approx$ 9.8	$\approx$ 10

BEARING DESIGN

Calculated bearing performance curves were obtained by use of the theoretical analysis for the spherical squeeze-film gas bearing with small steady-state radial displacement (Ref. 6). The pertinent design parameters of the experimental bearings are:

Azimuthal angle measured from the axis to the small diameter edge of the bearing (Φ_1)	40^o
Azimuthal angle measured from the axis to the large diameter edge of the bearing (Φ_2)	76.5^o
Clearance (c) based on difference in male and female member radii of curvature	0
Single-side axial end shake (δ_o) , mils	1.5
Radius of curvature (R), in	1.8

Performance curves of axial stiffness (k_Z), axial load capacity (F_Z) and radial stiffness for small radial displacements about the zero eccentricity position (K_R) are given in Figures 5 through 7 respectively. These curves are for the single end bearing. To obtain results for the double-ended float it is necessary to combine the effects of both ends.

The performance curves are based on the asymptotic squeeze-film solution which is applicable for large values of squeeze number, $\frac{12\mu V}{P_a}(R/C)^2$ greater than about 100. If the clearance (C) is taken as that due to end shake for the equivalent conical bearing (60 degree cone apex angle), the test bearing squeeze number is 275, so the asymptotic solution is applicable.

EXPERIMENTAL INVESTIGATION

Unmodified Transducer Design

The transducer, as originally designed, was assembled without the float in place and measurements of the bearing vibratory motion were made using Wayne-Kerr capacitance gaging equipment. The transducer was driven by an oscillator through a power amplifier with a multiple-tap output transformer. Current to the transducer was measured by sensing the voltage drop across a series resistor.

The drive frequency range from 4 to 40 kHz was surveyed and prominent resonances were identified at 13.5 kHz (Hoop mode), 4.9 kHz (axial mode), 5.25 kHz (axial mode) and 6.25 kHz (axial mode). There was a much weaker resonance of undetermined mode at about 24 kHz. A single male bearing member was readily floated with the transducer axis vertical at each of the three axial mode frequencies. Preliminary measurements of bearing element vibratory motion indicated considerable variation in amplitude with meridian angle.

In order to investigate bearing and transducer performance more fully, the float was assembled into the transducer with 0.0015 inch single-side axial end shake. With the axis vertical, the float was supported without difficulty at 4.9kHz drive frequency. Support was marginal at 5.25 and 6.25 kHz frequencies. When held with the float axis horizontal, the float support was at best marginal and, at worst, it would not lift at all. The performance depended on the direction of the gravity load vector with respect to the transducer assembly - that is, on the meridian angle of the load vector. Different values of axial end shake, including 0.001 and 0.002 inch single-side, were tried but these gave poorer, rather than better, results.

Capacitance gage probes were mounted on the float in order to measure the female bearing element motions with respect to the float in both the axial and radial directions. By turning the float, which was airborne, the variation in motion with meridian angle was determined. Results are given in Figures 8 and 9 for the two ends, identified as numbers 3 and 4 by the matching marks made on them during manufacture. The data are for a drive frequency of 4.9 kHz which was clearly the most effective of the several resonant frequencies with respect to achieving support of the float. The location and direction of the measurements are identified schematically. The angular position scale for both ends is based on clockwise meridional rotation from the reference mark when looking down on the No. 4 end.

These results show a very large (about 5 to 1) variation in the amplitude of the axial vibration with angular position. There is a similar variation in radial motion, especially when measured at the bearing segment, except that the maxima

for radial motion corresponds to the minima in axial motion. When the axial and radial motions are in phase, they are subtractive with respect to normal motion of the bearing surface. Thus, there was clearly a very large variation in squeeze-film excursion which could easily explain the rather unsatisfactory float lift characteristics of the transducer.

The transducer was disassembled and the piezoceramic cylinder was driven at its axial mode resonance. Measurements of the cylinder end motion indicated uniform motion of equal amplitude at all angular positions suggesting that the piezo-driver itself was not at fault.

As part of the subsequent effort to identify the reasons for the non-uniform motion of the bearing segments, measurements were made of the static stiffness of the flexure-bearing assemblies. The end assembly was supported on the annular surface which normally bears against the piezoceramic cylinder, and load was applied at the center of the male bearing member which was seated in the female bearing. Deflections were measured in the axial direction with respect to the surface of the support, which was a 1.5 inch thick block of steel. The deflections were measured at the step on the bearing and at the OD of the flexure washer, and at four equally-spaced positions around the ring corresponding to the 0, 90, 180 and 270 degree meridian angle positions. The results are shown in Figures 10 and 11. The deflection of both flexure sections is quite uniform with angular position and the two ends are comparable with an effective stiffness of about 3.5×10^6 lb/in. The deflection of the flexure section together with the connection between flexure and bearing sections is not so uniform, especially for the number 4 end. The measurements for this end show a variation in connection deflection with angular position of nearly 4 to 1. The point of lowest connection deflection is close to the reference mark which corresponds to the region of maximum vibratory motion of the assembled transducer (Figure 9). For the number 3 end, the variation is much smaller and may be within the range of measurement error. Thus, it appeared likely that the observed nonuniformity in the bearing excursion was caused by the meridional variation in flexure-to-bearing connection stiffness of the number 4 end.

MODIFIED TRANSDUCER DESIGN

The transducer design was modified as shown in Figure 4 to obtain a stiffer, more uniform connection between the flexure and bearing sections. Since this required fabrication of new flexure sections, the flexure washer thickness was also increased from 0.170 to 0.190 inch in an effort to obtain a flexure stiffness closer to the design objective of 5.0×10^6 lb/in. Prior to assembly, the surfaces of the flexure-bearing connection were lapped together.

Static compliance of the flexures and of the combined flexure-bearing sections were measured as before. The results showed uniform flexure deflections with an overall flexure stiffness of 5.0×10^6 lb/in. Deflection of the combined flexure and connection, measured at the bearing step, showed variations at the four, equally spaced angular positions of about 10 percent which is within the estimated experimental error.

The transducer was assembled in a step-wise fashion and performance was checked at each step. With just the flexure sections attached to the driver, and with the tie bolts installed and the driver-flexure connections epoxy filled, the unit drove extremely well at 7.8 kHz. The motions, measured at the end surface which bears against the bearing seqment, were uniform within 10 percent and the system obviously had an extremely high mechanical Q. Axial excursion amplitudes in excess of 700 μ in p-p were obtained with 40 volts rms drive.

Attaching the bearing sections brought the resonant frequency down to 5.75 kHz; reduced the mechanical Q substantially; and produced significantly smaller motions as measured at the bearing steps. The performance of the modified transducer without the float is summarized in Figure 12. The variation in axial excursion amplitude with angular position was much less than that obtained with the unmodified transducer, but there were still differences of about 20 percent. Radial motions were measured outboard from the bearing step (position B as shown in the schematics of Figures 8 and 9). These measurements showed a radial, hoop mode vibration coupled to the axial excursion and in phase with it - that is, as the female bearing moved outward, away from the center plane, it also expanded, becoming larger in diameter.

The interaction of the axial and hoop mode vibrations is such that they are subtractive insofar as the squeeze motion normal to the bearing surface is concerned. The effect is substantial, particularly at the large diameter end where the actual normal surface excursion is apparently only about 50-60 percent of that which would prevail if there were no hoop mode motion. There was no accessible surface for measurement of motion in the radial plane at the small diameter end with the modified transducer design. However, previous measurements on the unmodified transducer (Figures 8 and 9) suggest that there are no modal points along the bearing element and the radial motions at the small diameter end are nearly as large as those measured at the large diameter end.

The float was assembled into the transducer and measurements were made of the bearing axial excursion with respect to the float (Figures 13 and 14). The addition of the float resulted in a general, overall reduction in axial excursion amplitudes (by a factor of about 1.8 which is somewhat larger than the reduction previously noted for the conical bearing. However, it should be noted that only one male bearing part was used with the conical bearing transducer.) In addition, there appears to be a greater variation in the excursion with meridian angle (up to about 35 percent from the previously observed 20 percent). In part, these effects are believed to be manifestation of additional damping introduced by the bearing squeeze films. They probably also reflect the fact that axial vibratory motions of the float were detected at the squeeze frequency. The float motion, or more properly, the motion of the male bearing segment attached to the float, was measured by a capacitance probe supported on a holder resting on the table surface. The motion was in phase with the female bearing axial excursion and it amounted to about 10 percent of the female bearing axial excursion measured with respect to the male bearing (40 μ in p-p float motion at 100 volts rms drive with a female bearing axial excursion of about 350 μ in p-p). The effect of the male bearing vibration is to reduce the effective squeeze-film excursion ratio. It's significance is indicated by the fact that reducing the excursion ratio by ten percent, from $\epsilon = 0.55$ to $\epsilon = 0.5$, reduces the theoretical load capacity and stiffness by 15 to 20 percent.

Axial and radial load capacity measurements of the complete float squeeze-film support were obtained by suspending weights from the float and measuring the

resulting displacement using capacitance probes mounted on the float "looking at" the female bearing. The single bearing axial load capacity, calculated from the theoretical data of Figure 6, is shown in Figure 15 for 250 and 127 μ in single-side axial excursions. The 127 μ in excursion data represents an equivalent axial excursion for combined axial and hoop mode vibrations of 250 and 70.5 μ in single-side amplitudes respectively. The correction is approximate since it presumes uniform amplitude vibrations and a single value of the normal component of the hoop mode motion based on a 60 degree apex angle conical bearing surface. Calculated and measured axial load capacities for the complete float are given in Figure 16. The measured data points (140 v rms drive) lie between the two calculated curves suggesting that, while some correction in the excursion based on measurement of axial motion alone is needed, the correction used was too extreme. The measured ultimate load capacity, defined as the maximum load which could be supported before there was evidence of contact between the bearing surfaces, was 12.65 lb. axial and 6.65 lb. radial.

Complete theoretical data for calculating radial load capacity were not available. However, the calculated radial stiffness for small excursions about the zero radial eccentricity position is 12.6×10^3 lb/in. for an axial excursion amplitude of 250 μ in single-side and 6.6×10^3 lb/in. for the corrected axial excursion of 127 μ in. Based on the observed radial deflection due to the 1.65 lb. float alone (difference in float radial position with the axis horizontal and vertical), the measured radial stiffness was 5.9×10^3 lb/in. at the number 3 bearing end and 5.4×10^3 lb/in. at the number 4 end. Thus, the radial load results show much better agreement with those calculated results which include the correction to the excursion for hoop mode vibration. It appears that the coupled hoop mode vibration has a greater effect on the bearing performance with radial loading than it has with axial loading. This is reasonable for the spherical bearing geometry since at the large diameter section of the bearing there is both a greater projected area for radial loading and a larger effect of hoop mode vibration on the normal squeeze motion of the surface. It seems likely that the hoop mode motion at the small diameter end of the bearing would be smaller than that measured at the large diameter end because of the much greater section thickness there. This plus the reduced radial motion component in the direction normal to the surface (because of the spherical geometry) would mitigate the loss in performance with axial loading.

The measured radial stiffness based on the deflection resulting from increasing the radial load from 5.65 to 6.65 lb. was 12.5×10^3 lb/in. at the number 3 bearing and 13.0×10^3 lb/in. at the number 4 end. These data were obtained with the radial load vector passing through the 180 degree meridian angle position.

CONCLUSIONS

1) The performance of the spherical-bearing, axial-excursion transducer as a support for the simulated gyro float was generally satisfactory. For idealized squeeze motion, the experimental device failed to match the theoretical float load capacity and support stiffness characteristics by a factor of roughly 2 for axial loading. Based on radial stiffness for small displacements about the zero radial load position, the discrepency for radial loading was about the same with measured stiffnesses of 43 and 47 percent of theoretical for the two ends measured separately. The maximum loads which could be carried without apparent contact between the bearing surfaces were 12.65 and 6.65 lbs. for axial and radial loads respectively.

2) The idealized squeeze motion, as assumed in the theoretical work, is a uniform, rigid body, axial excursion of the female bearing elements. The actual motion differed from this idealized model in several respects.

   (a) The axial motion was not uniform - instead there were variations in amplitude with meridian angle of 20 to 35 percent.

   (b) There is a hoop mode vibration of the female bearing element coupled to the axial excursion such that the squeeze motion measured normal to the bearing surface, is reduced by the interaction. The effect on bearing squeeze motion appears to be significant, particularly at the large-diameter end of the bearing. In this region the actual, normal squeeze motion is only about 50 percent of that which would be obtained if there were no coupled hoop mode motion.

3) When an approximate correction was made to the axial excursion used in the calculations for the effect of the coupled hoop mode vibration, the measured and calculated results were in good agreement for radial loading. The correction brought the calculated performance for axial loading below the measured performance by a margin nearly equal, but opposite to that obtained for idealized squeeze motion. These apparent differences in the effect of the

coupled hoop mode motion with load direction can be explained by the spherical geometry of the bearing surface and the probability of reduced hoop mode amplitude at the small-diameter end of the bearing.

4) The maximum radial load is only about half the maximum axial load. This may be in part due to the fact that the male and female bearings were lapped uniformally and consequently the radial clearance is smaller than the axial clearance, the latter having been adjusted for best axial load capacity. It is quite possible that the radial load capacity can be improved without impairing the axial load capacity if the female bearings could be lapped to a radius slightly larger than that of the male bearings.

5) The preceeding observations apply to the modified transducer design. The modification was aimed at achieving greater, more uniform stiffness of the connection between the flexure and bearing sections by changing from an interface loaded in shear to one loaded in direct bearing. Prior to the modification, the axial excursion of the bearing element was extremely nonuniform - differences in amplitude of as much as 1 to 5 depending on angular position. The modification was very helpful, but it has become clear that connections between parts, especially outboard from the flexures, are extremely critical. Such connections are very likely to sharply reduce the mechanical Q of the system, presumably because they introduce damping. They are also very likely to cause meridional nonuniformity of the bearing element axial excursion. In this regard it is worth noting that there was no evidence of this type of nonuniformity in the motion of the earlier one-piece conical bearing transducer, although that unit did have nonuniformity of motion due to a coupled twisting motion of the bearing cross section. The two-piece design with separate, connected flexure and bearing sections was chosen to obtain a bearing element which was resistant to cross-sectional twisting, yet light enough to keep the system resonant frequency reasonably high and, at the same time, to have the flexure made of a material of high strength and low internal damping. On balance, the one-piece design is probably to be preferred because of greater long-time reliability and more predictable, consistent performance. Also, if there is to be nonuniformity of the squeeze

motion, and it seems that there will be, it is probably preferrable for it to be a mode yielding uniform excursion about the axis, such as twisting of the bearing cross section. The meridional mode of nonuniformity observed with the two-piece design, is more undesirable because it should produce nonuniform radial stiffness of the float support.

6) The design charts for the axial-excursion squeeze-film transducer (Ref. 3) were accurate in the prediction of operating frequency of the experimental transducer after the modification to improve connection stiffness was made. There was no experimental confirmation of the calculated amplification factor since the driver section excursion was not measured.

7) One reason for preferring the spherical bearing over the conical was its insensitivity to alignment of the two bearing ends. This expected advantage was realized since there were no unusual precautions taken to insure alignment and there was no evidence of operational difficulty attributable to misalignment effects.

8) The triangular frame support for the transducer was satisfactory and it offered very little apparent restraint to the piezoceramic tube driving motion.

9) There was no evidence of material transfer or surface deterioration of the annodized aluminum bearing elements.

LIST OF REFERENCES

1) "Analysis, Design and Prototype Development of Squeeze-Film Bearings for AB5 Gyro - Phase I Final Report, Bearing Analysis and Preliminary Design Studies", edited by C.H.T. Pan, MTI-64TR66, Contract NAS8-11678, 1964.

2) Pan, C.H.T., Orcutt, F.K., and Teitelbaum, B., "Analysis, Design and Prototype Development of Squeeze-Film Bearings for AB5 Gyro - Phase II Final Report, Fabrication and Evaluation of Floating-Transducer Squeeze-Film Bearing Prototype", MTI-67TR17, Contract NAS8-11678, 1967.

3) Chiang, T., and Pan, C.H.T., "Analysis and Design Data for the Axial Excursion Transducer of Squeeze-Film Bearings", MTI-65TR25, Contract NAS8-11678, 1965.

4) Orcutt, F.K., Kissinger, C., and Pan, C.H.T., "Investigation of an Axial-Excursion Transducer for Squeeze-Film Bearings", MTI-65TR63, Contract NAS8-11678, 1965.

5) "Bearing Performance Measurements for 45 degree Cone, Squeeze-Film Transducer with Precision Ground Surfaces", attachment to Progress Report No. Twenty-Two, Contract NAS8-11678, Covering June, 1966.

6) Chiang, T., Malanoski, S.B., and Pan, C.H.T., "Spherical Squeeze-Film Hybrid Bearing with Small Steady-State Radial Displacement", MTI-65TR30, Contract NAS8-11678, 1965.

APPENDIX A

EXPERIMENTAL INVESTIGATION OF NASA BUILT SQUEEZE-FILM BEARING TRANSDUCER

This transducer bearing assembly had been used as a demonstration unit prior to its receipt at MTI for evaluation. In the course of the demonstrations the performance of the unit had changed, for the worse, and when received it was not operating as well as it had previously. Nevertheless, measurements of transducer performance were undertaken to determine the mode of squeeze motion and, insofar as possible, the performance characteristics. During these measurements, the following observations were made:

1) When driving with the self-tuning circuit, the unit did not operate at resonance (there was only a small current draw and small vibration amplitudes). Replacing the self-tuning circuit with a manually tuned driver, two major system resonant frequencies were found in the range of 38-41 KC. The self-tuning circuit was driving between these two resonant frequencies.

2) Using the manually-tuned driver, it was observed either male bearing segment could be floated at one end (the left end as identified on the accompanying sketch) and neither would float in the right end bearing.

3) Removing the float and using a fiber-optic sensor to measure motion at the bearing O.D., one strong resonant frequency was found (identified by a peak in measured vibration amplitude) at 40,400 $\pm$ 50 cps for the left end. At the right end, there were a number of resonant frequencies in the range of 38,300 to 40,400 cps. The vibration amplitudes of each of these resonant frequencies were roughly equal and all were of considerably smaller amplitude than was obtained at the left end at 40,400 cps. From this and the fact that there is an audible vibratory noise when driving the unit, it appeared that the integrity of the driver-bearing connection at the right end has probably been damaged.

The fiber-optic sensor was used to measure motions at various points on the

left-end bearing when operating at the 40,400 cps resonance. The locations of the measurement points are indicated at the bottom of the attached sketch. The results of these measurements are summarized as follows:

1) The motion amplitudes are large at the outer, large diameter, end (measurement point A) and decrease steadily as the probe is moved inward. Specifically for 20 volts runs drive, the measurements normal to the bearing surface are as follows:

Position	Motion Amplitude μ in p-p
A	185
B	40
C	< 10 μ in
D	(Comparable to the instrument noise level)

A slot was milled through the outer housing at one position to provide access for measurements on the outer surface of the bearing section. With 20 volts rms drive, these are:

Position	Motion Amplitude μ in p-p
E	90
F	23
G	10-15
H	< 10

2) Measurements at four, equally spaced angular positions at the O.D., position A, showed the motion to be in phase and equal at each point. From this, and the results described in 1, it appears that the transducer operates with a hoop mode vibration of the bearing section with large amplitudes in the thin, large diameter region and very little motion at the heavy section near the connection to the flexure. Alternatively, it is possible that the mode is a rotation of the entire section with a nodal point near the flexure connection.

In any case, it is clearly not an axial mode vibration of the bearing section as a rigid body connected to the flexure.

3) Vibration amplitude, measured at point A (normal to the bearing surface at the large diameter end) and transducer power consumption were measured at 40,400 cps frequency for several values of drive voltage. Results are as follows:

Drive Volts, rms	Motion Amplitude μ in p-p	Power Watts
10	110	1.3
20	195	4.6
30	430	12.6

Fig. A-1

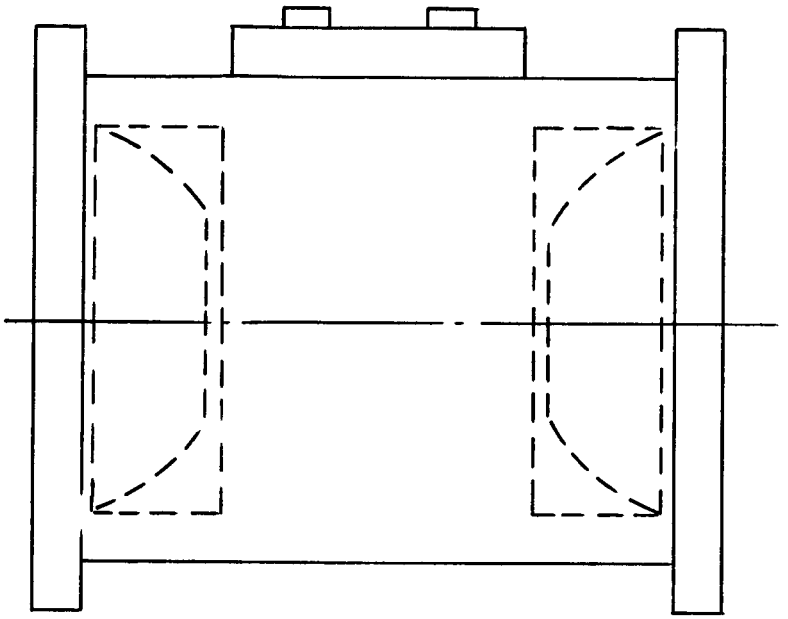

Fig. A-2

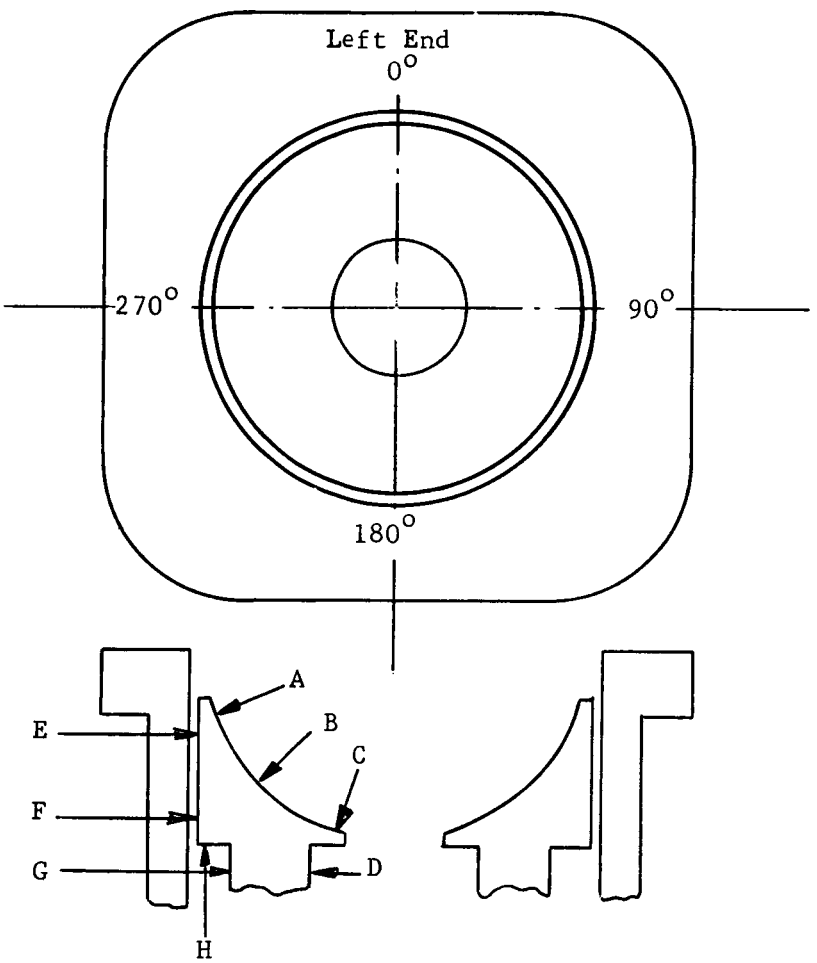

LIST OF SYMBOLS

C Bearing clearance equal to difference between female and male segment radii of curvature, in.

e Axial excursion, single-side peak, in.

F_z Axial load, lb.

P_a Ambient pressure, $lb/in.^2$

K_R Radial stiffness, lb/in.

K_z Axial stiffness, lb/in.

R Bearing radius of curvature, in.

δ Bearing single-side axial end shake, in.

Λ Compressibility number = $\frac{6\mu\omega}{P_a} (R/C)^2$

μ Viscosity, $lb.sec/in.^2$

ν Squeeze frequency, rad./sec.

φ Azimuthal angle between bearing edge and center axis, degrees.

ω Meridional angular speed of rotation, rad./sec.

LIST OF FIGURES

13) Axial Excursion Measurements for Modified Transducer - No. 3 Bearing End, Float Installed.

14) Axial Excursion Measurements for Modified Transducer - No. 4 Bearing End, Float Installed.

15) Calculated Axial Load Capacity of Experimental Spherical Squeeze-Film Bearing - Single End.

16) Calculated and Measured Float Axial Load Capacity.

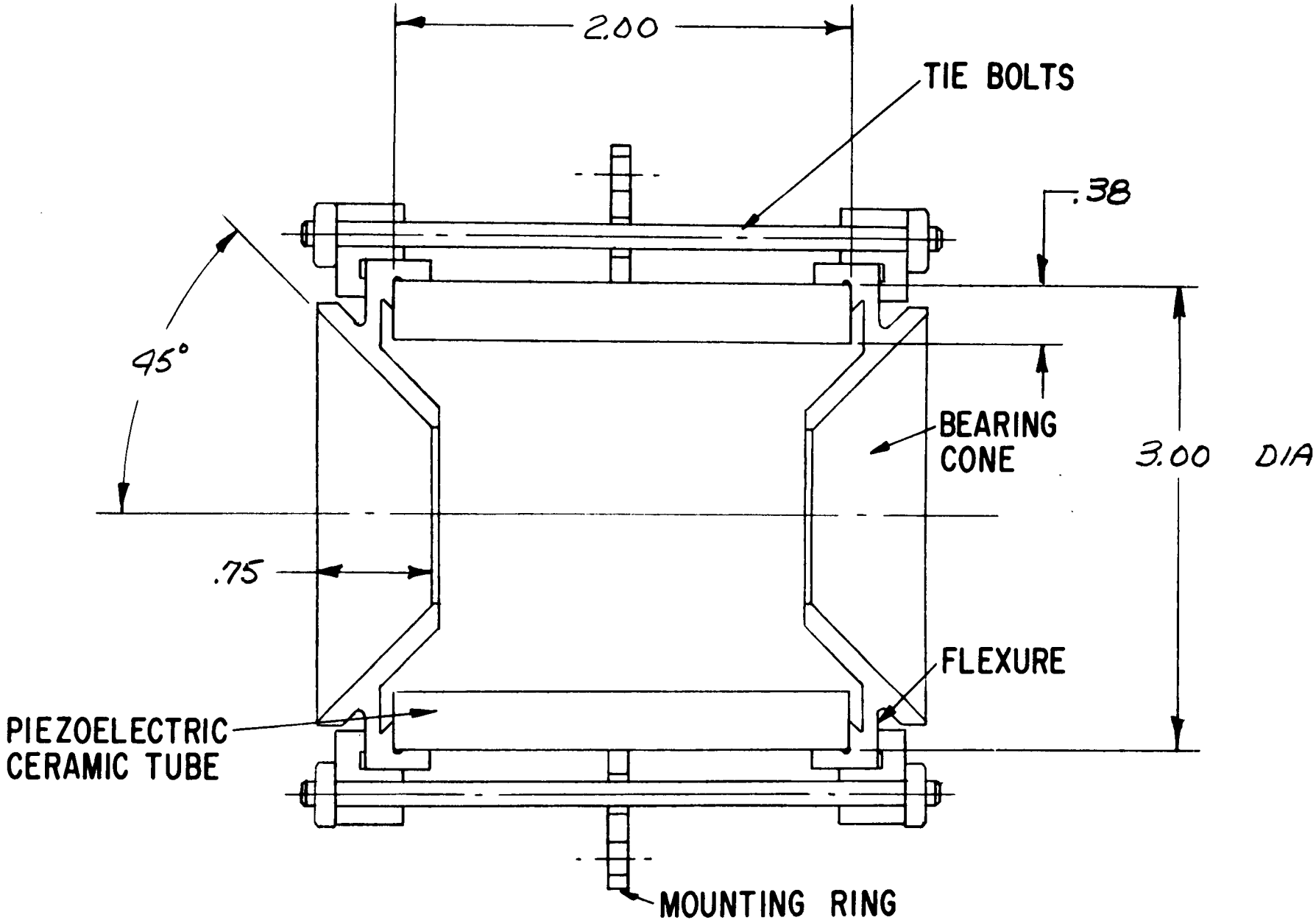

Fig. 1 Experimental Conical Bearing, Axial-Excursion, Squeeze-Film Transducer Assembly MTI-2940

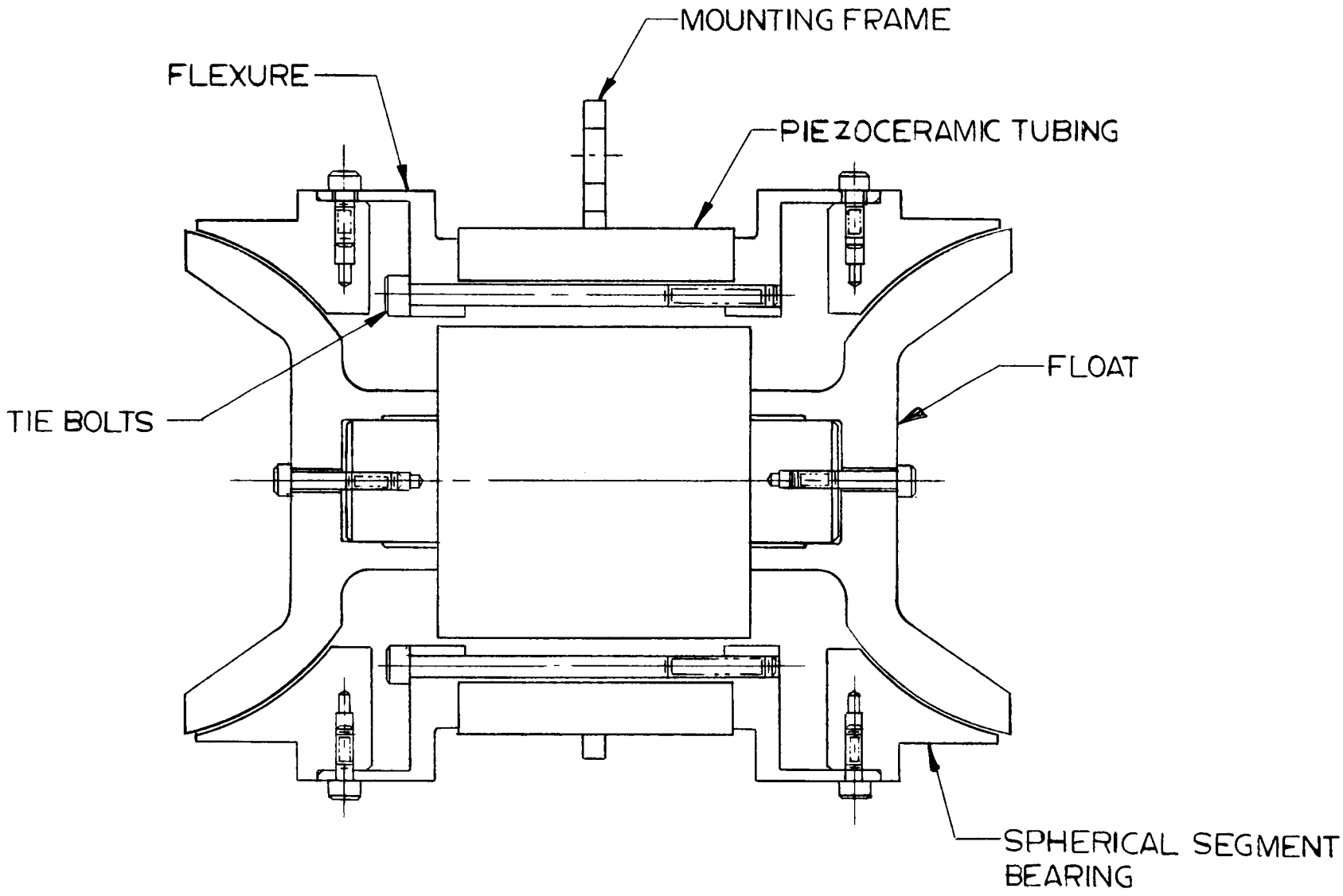

Fig. 2 Cross Sectional View of Unmodified Spherical-Bearing, Axial-Excursion Squeeze-Film Transducer.

MTI-3042

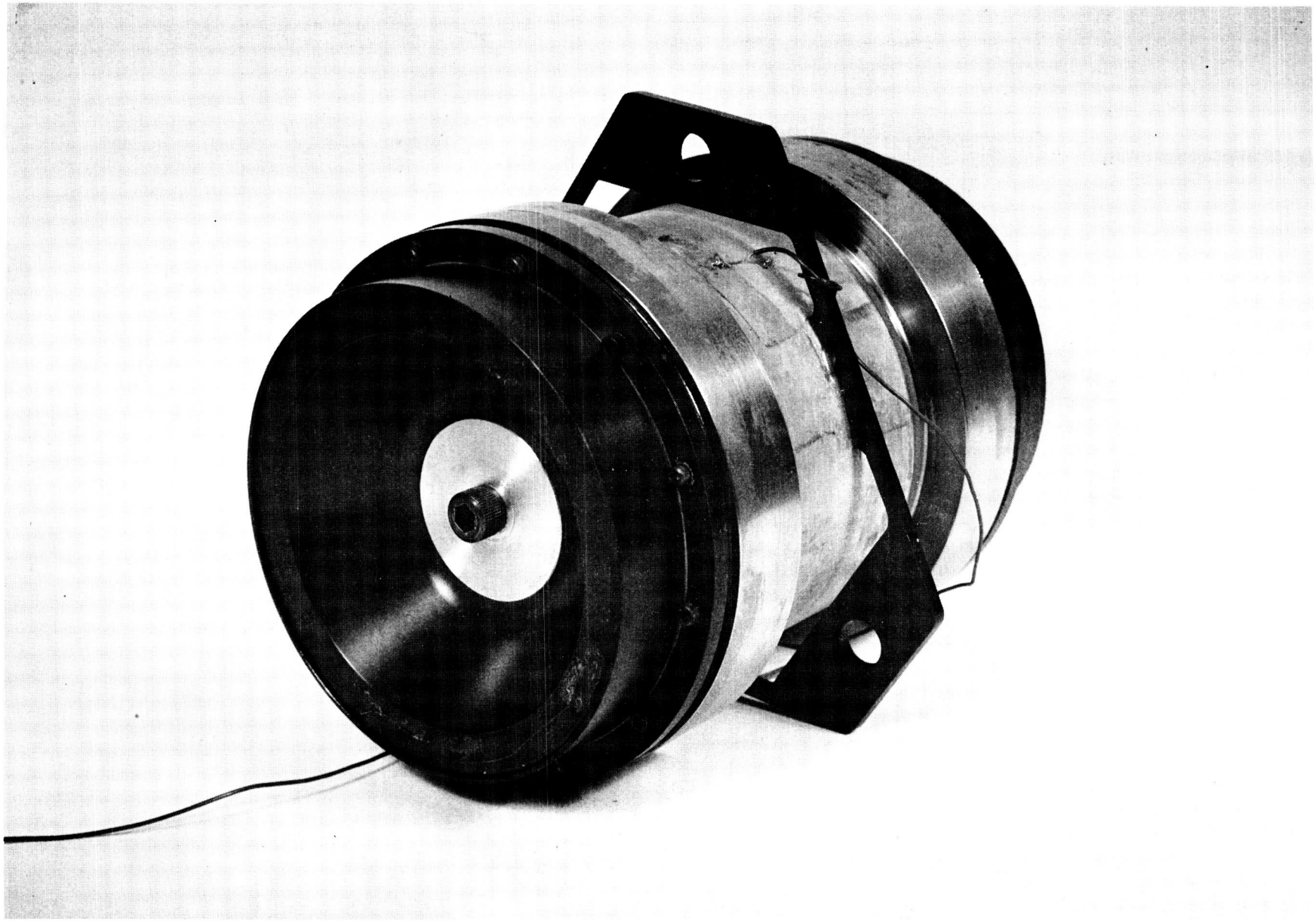

Fig. 3 Spherical-Bearing Prototype with Assembled Float

MTI-3043

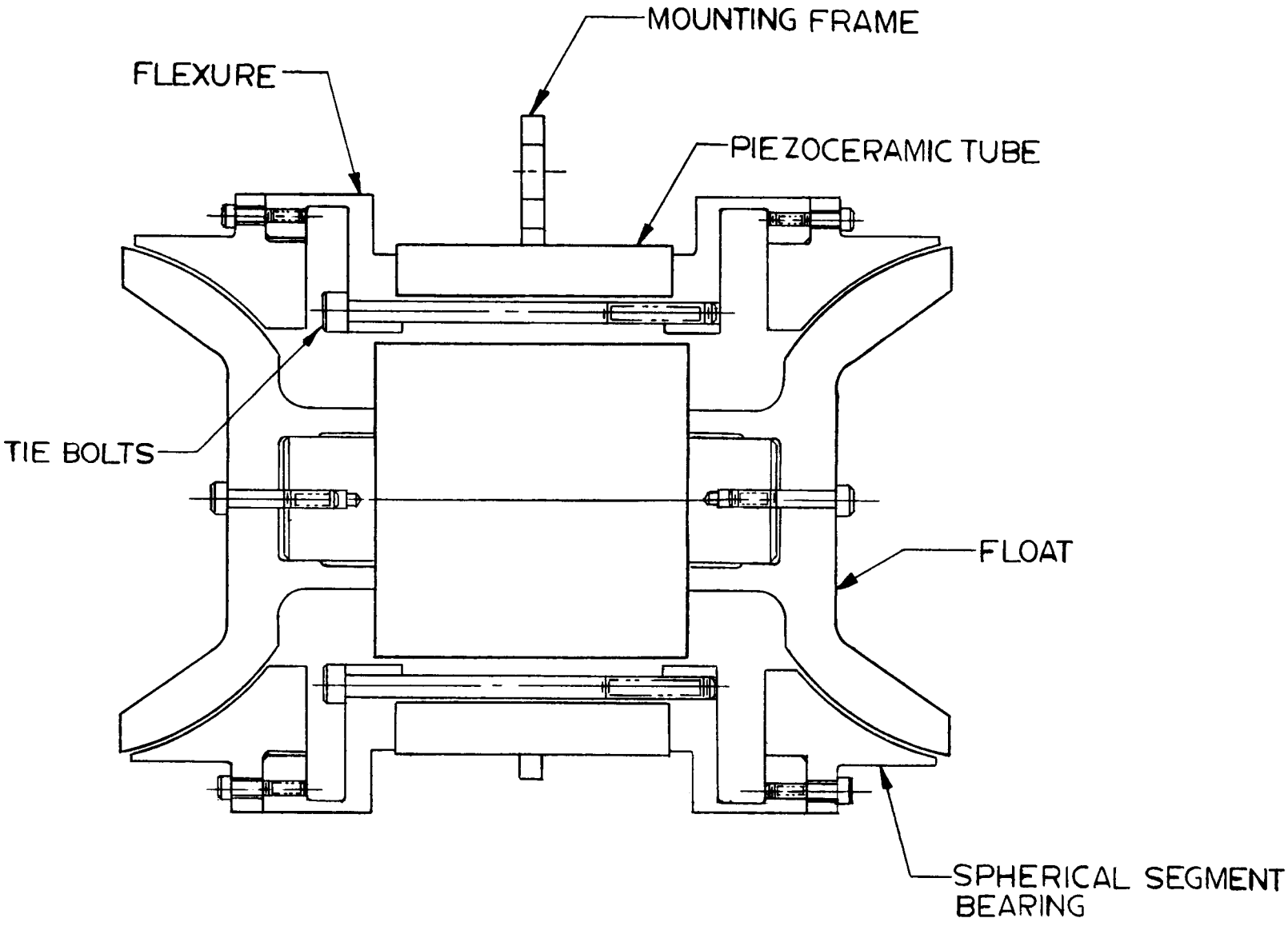

Fig. 4 Cross Sectional View of Modified Spherical-Bearing, Axial-Excursion Squeeze-Film Transducer.

MTI-3044

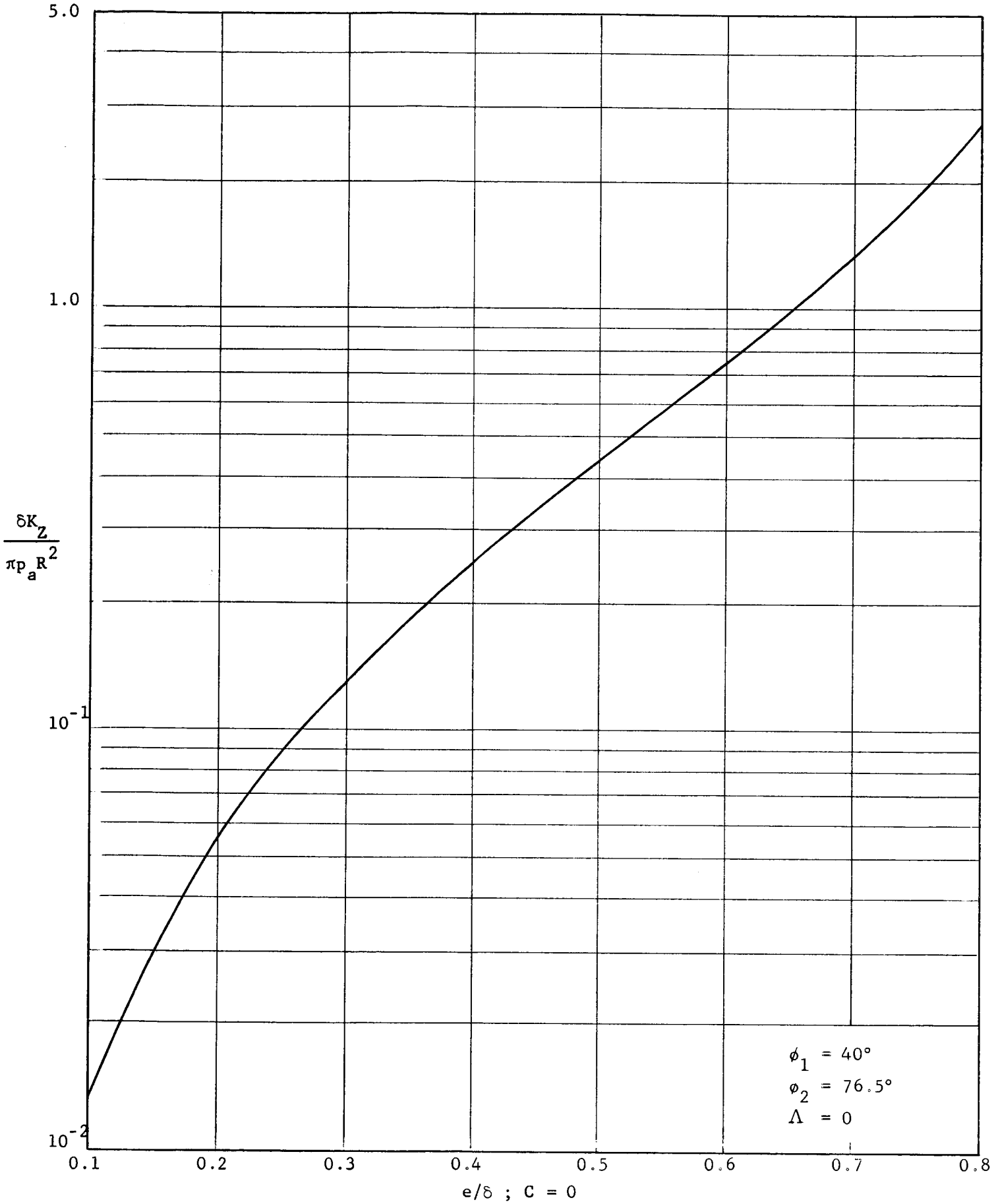

Fig. 5 Axial Stiffness vs. Excursion Ratio for Spherical-Bearing Prototype - Single End

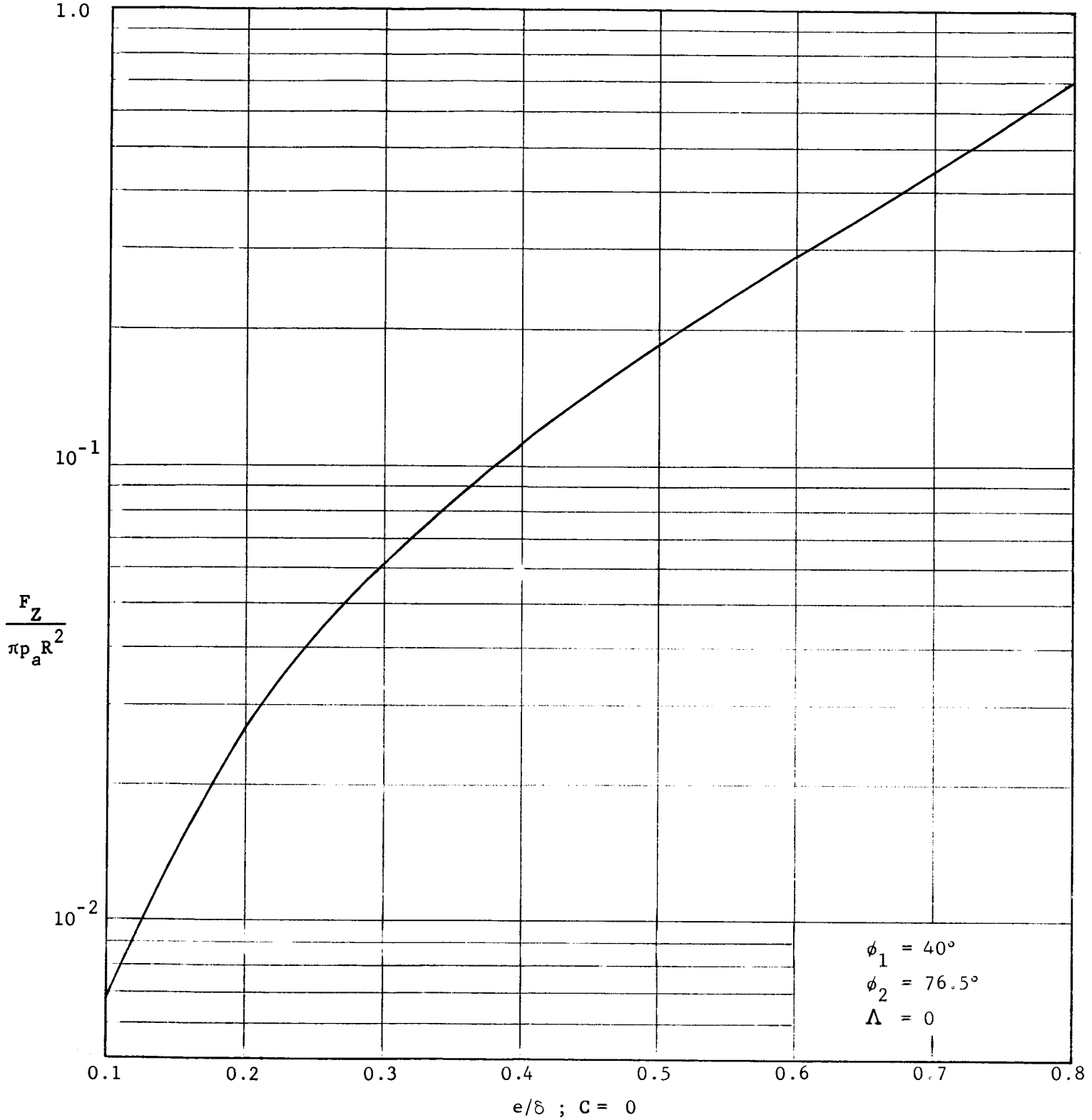

Fig. 6 Axial Load Capacity vs. Excursion Ratio for Spherical-Bearing Prototype - Single End

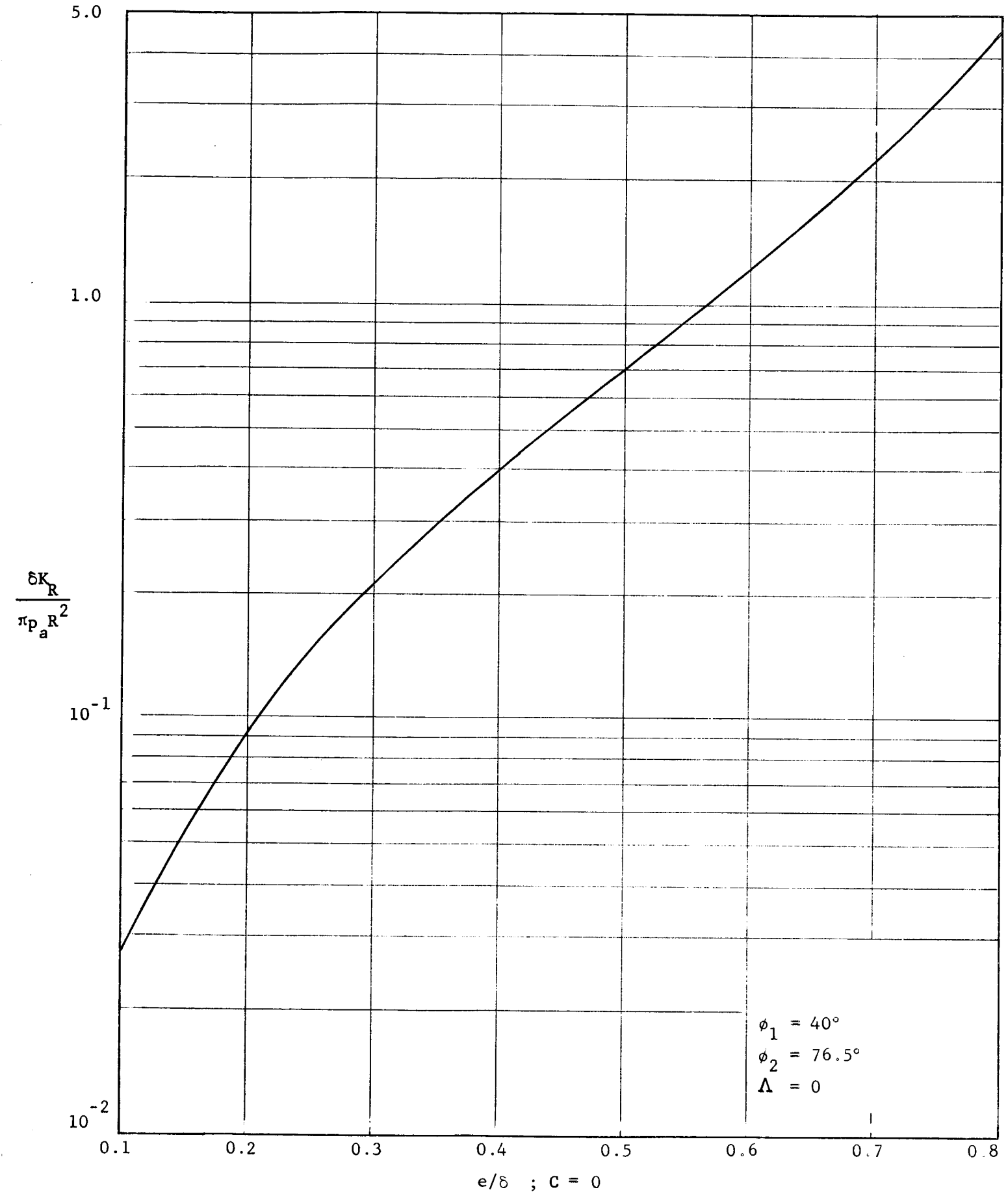

Fig. 7 Radial Stiffness for Small Steady-State Displacements vs. Excursion Ratio for Spherical-Bearing Prototype - Single End.

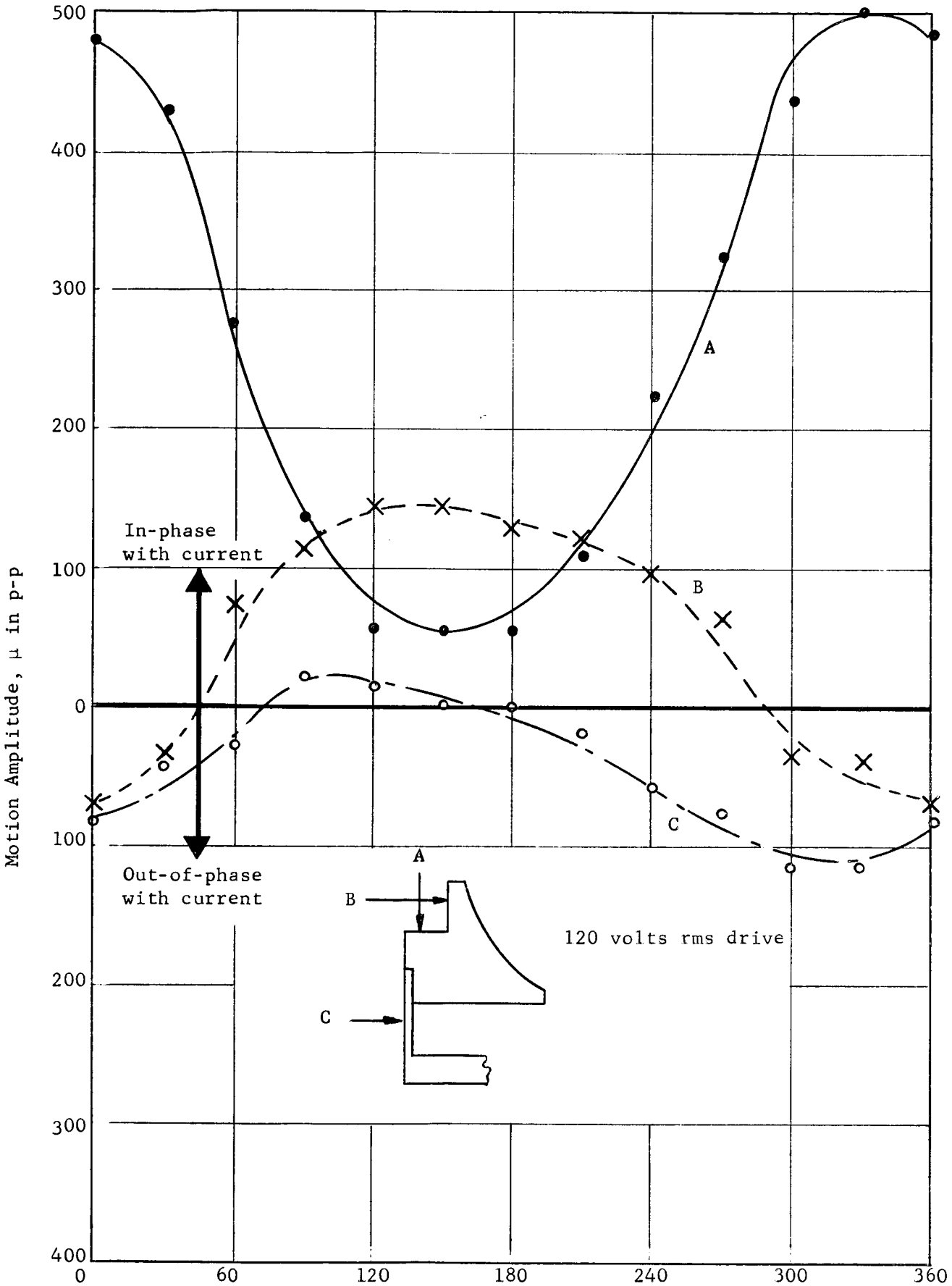

Fig. 8 Measured Vibratory Motions _ Unmodified Transducer With Float Assembled - No. 3 Bearing End

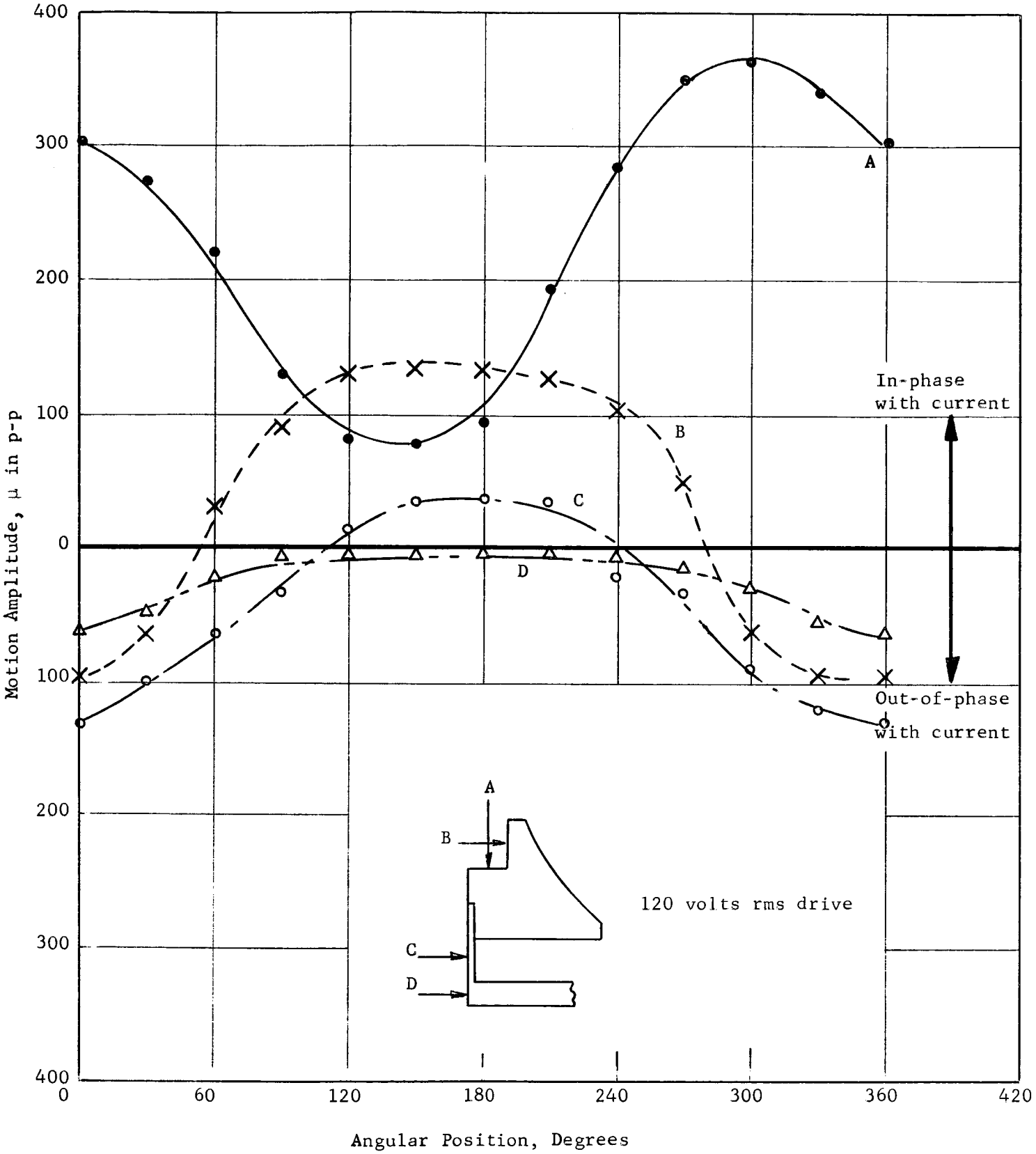

Fig. 9 Measured Vibratory Motions — Unmodified Transducer With Float Assembled — No. 4 Bearing End

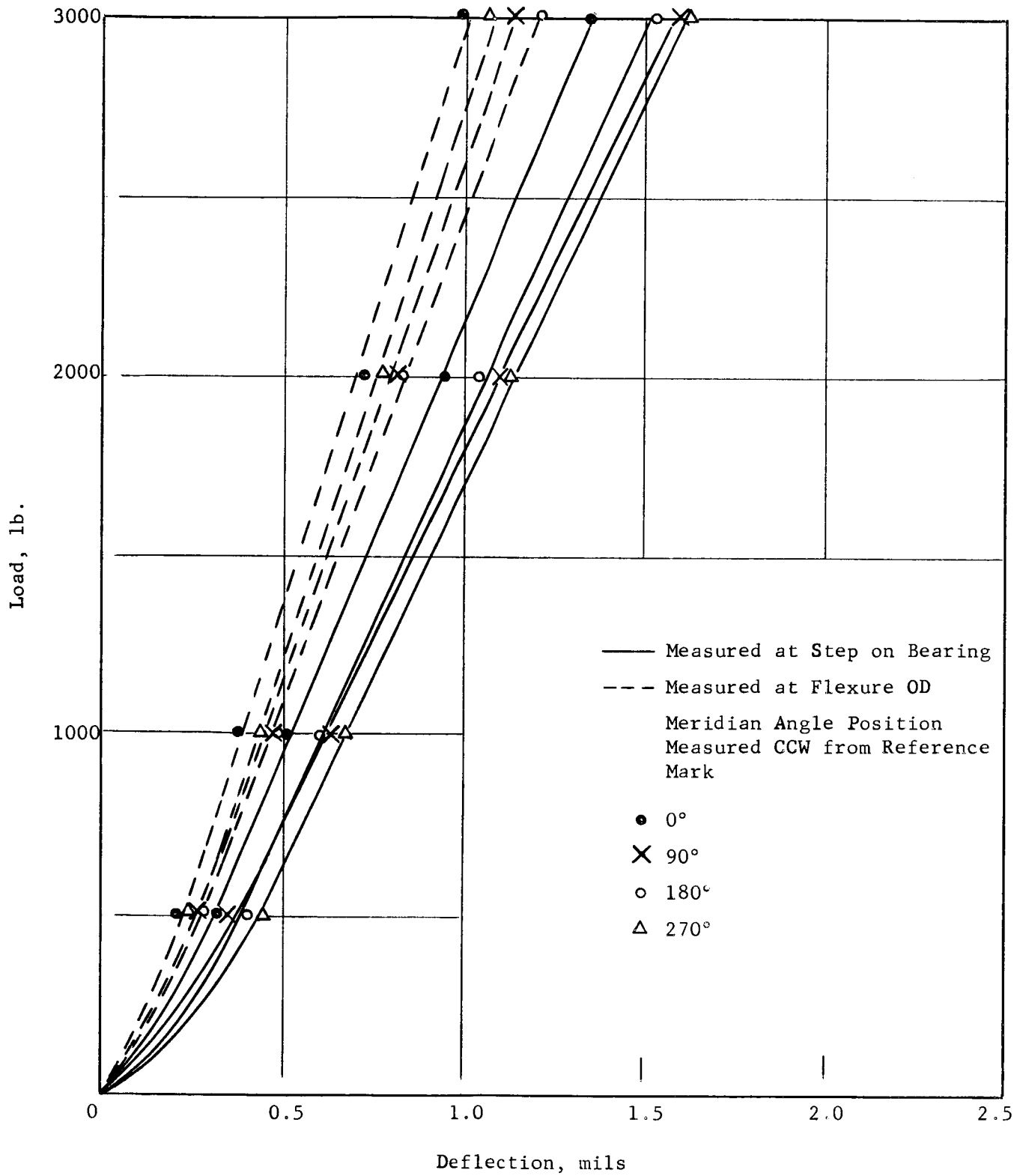

Fig. 10 Static Deflection of No. 3 Spherical-Bearing End — Unmodified Design

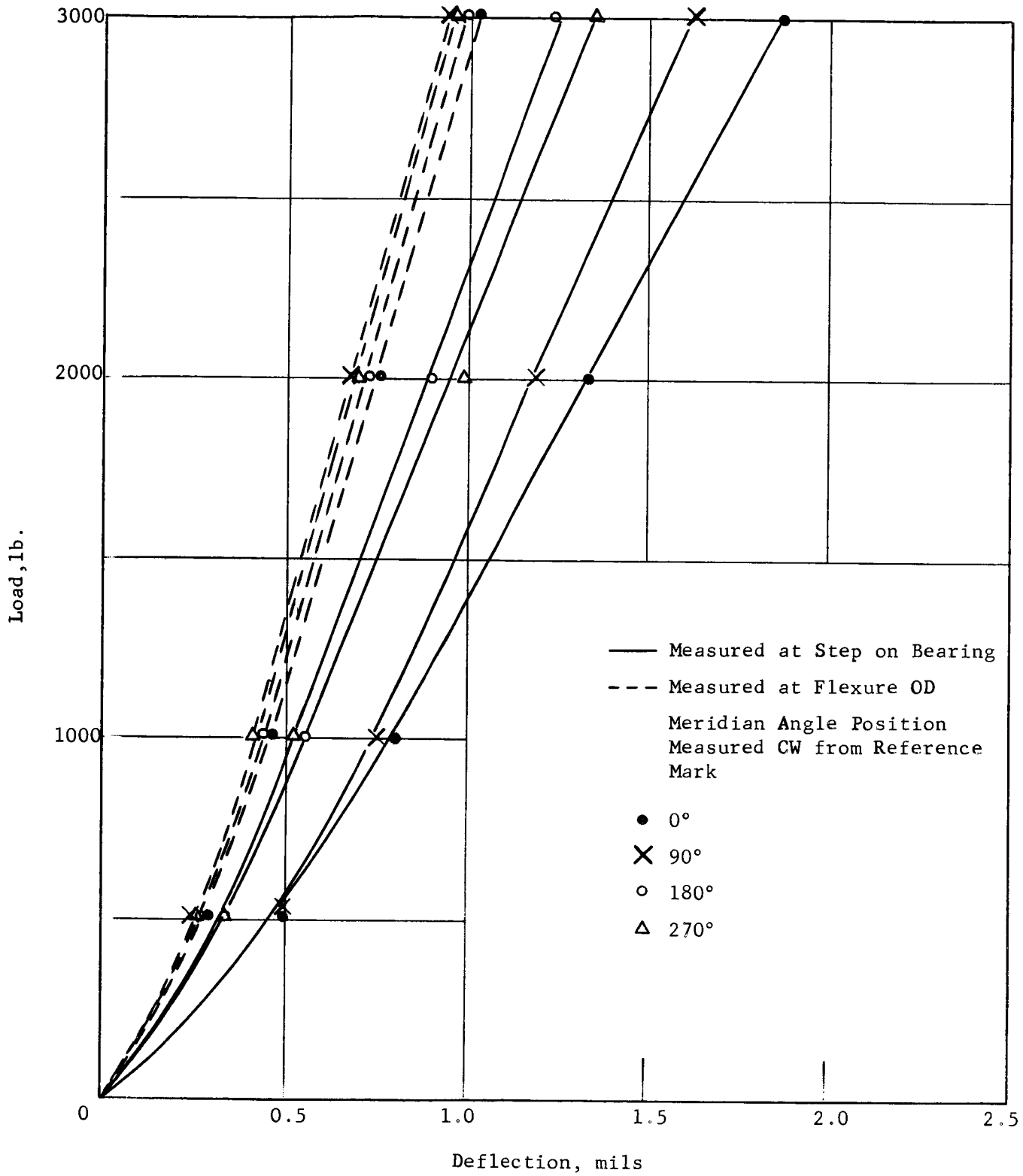

Fig. 11 Static Deflection of No. 4
Spherical-Bearing End —
Unmodified Design

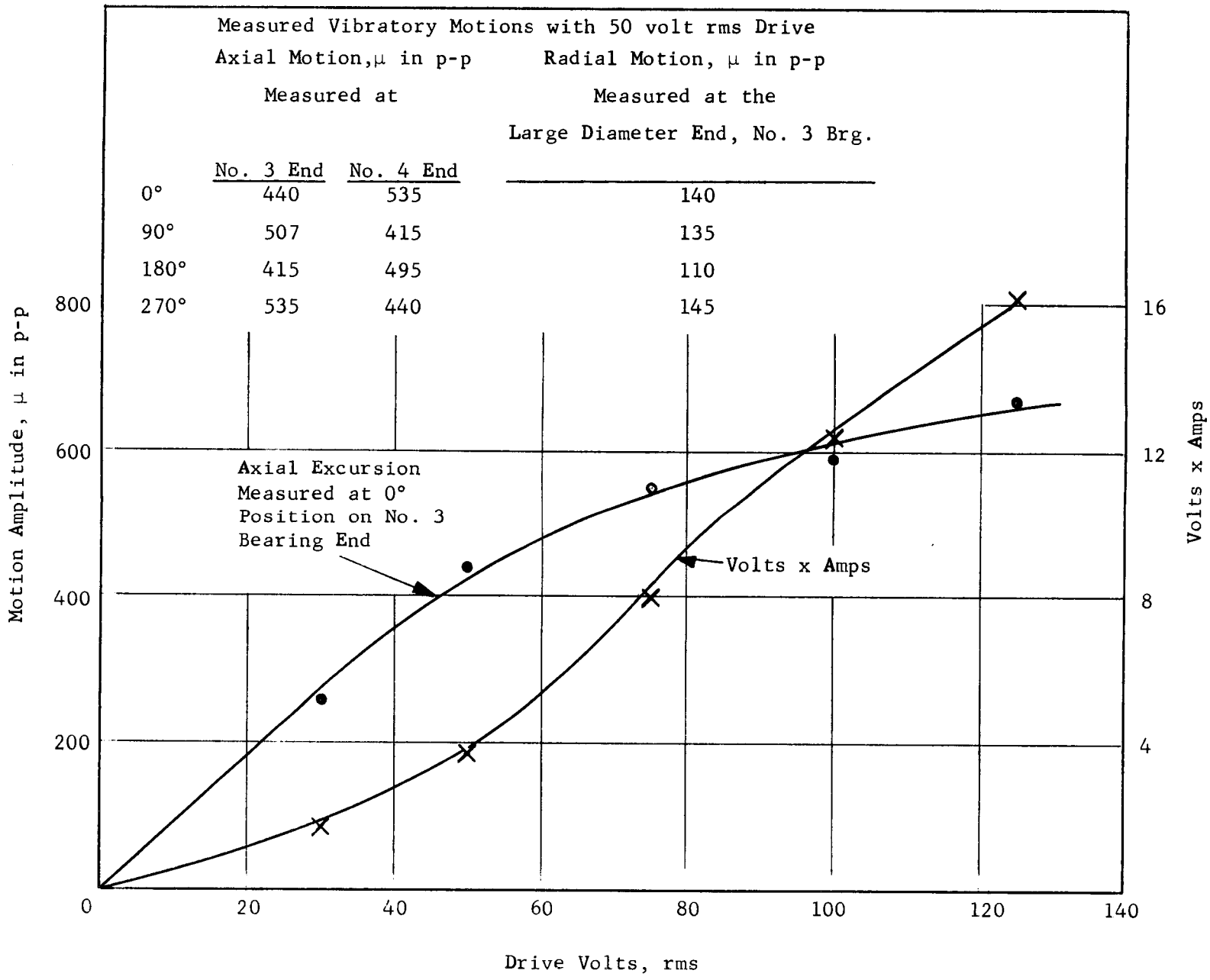

Fig. 12 Performance of Modified Transducer Without Float

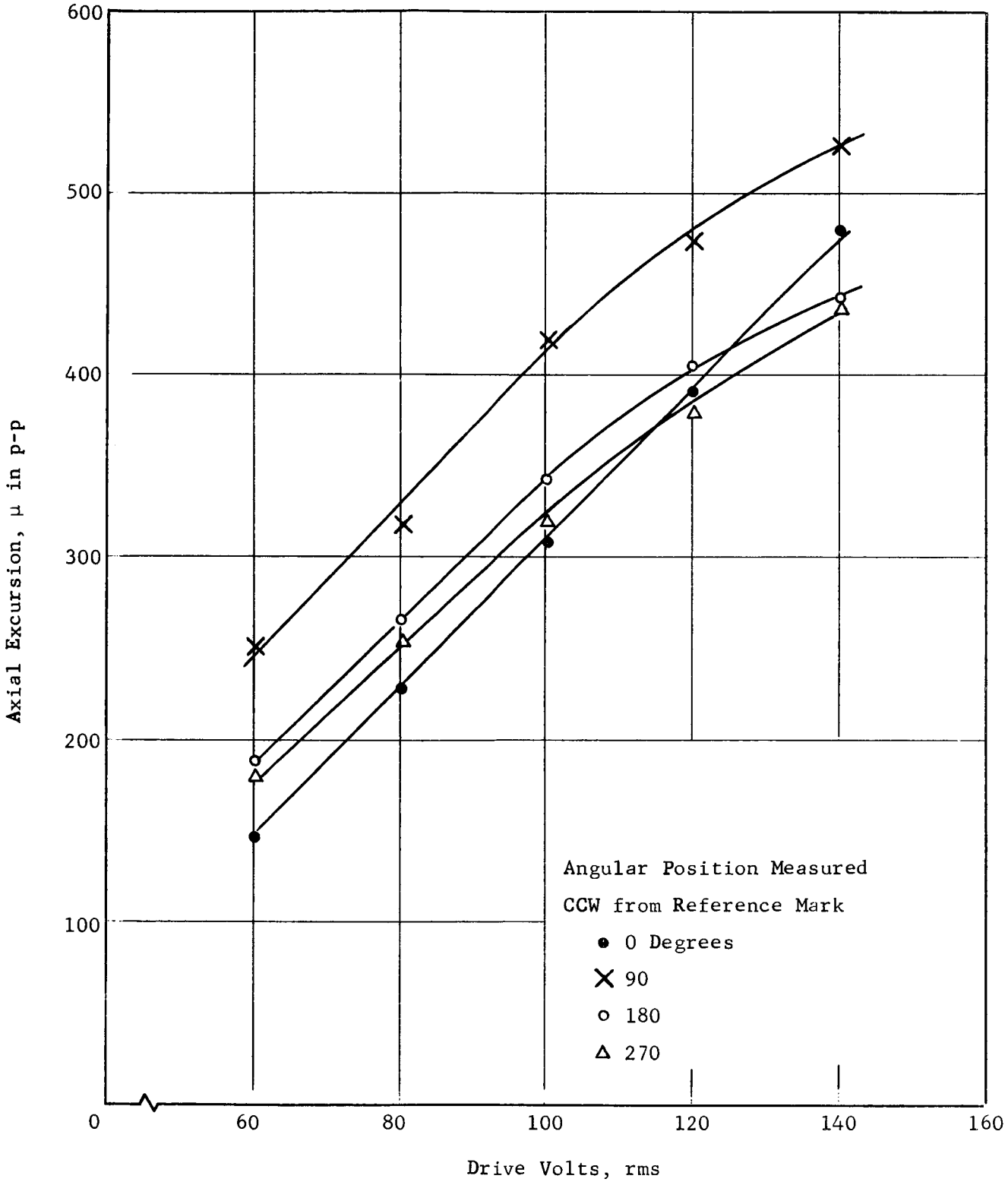

Fig. 13 Axial Excursion Measurements for Modified Transducer No. 3 Bearing End, Float Installed

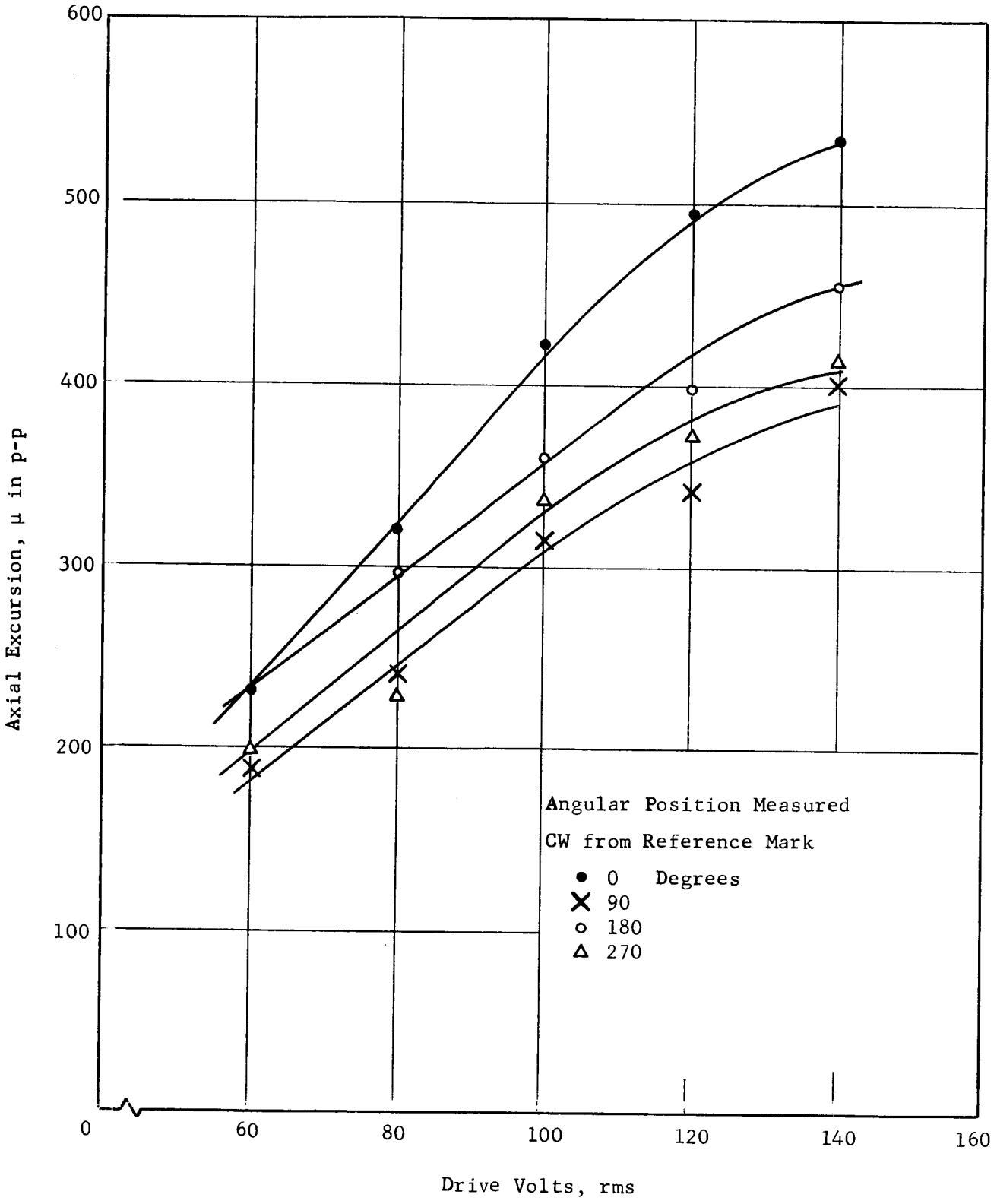

Fig. 14 Axial Excursion Measurements for Modified Transducer No. 4 Bearing End, Float Installed

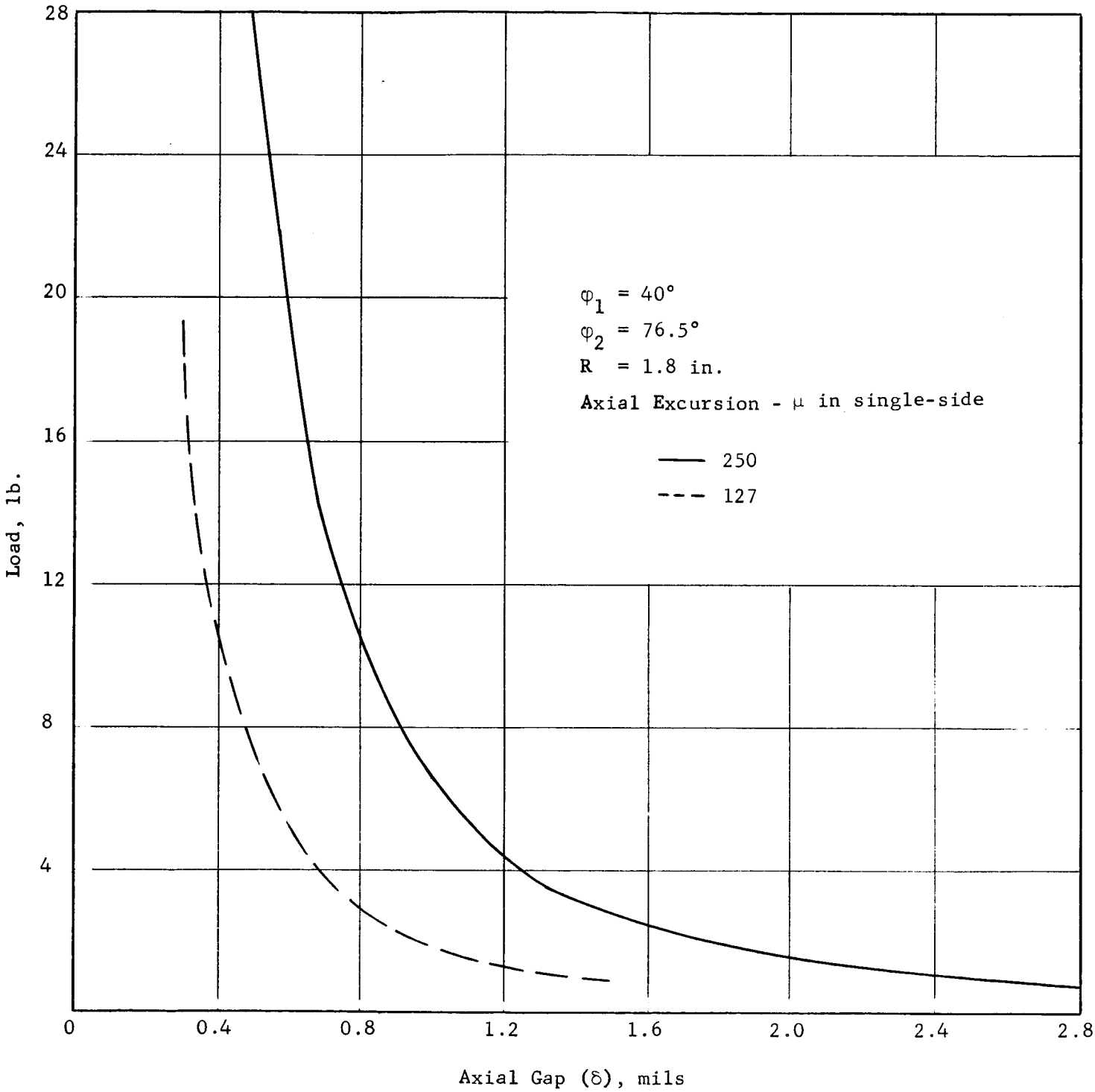

Fig. 15 Calculated Axial Load Capacity of Experimental Spherical Squeeze Film Bearing - Single End.

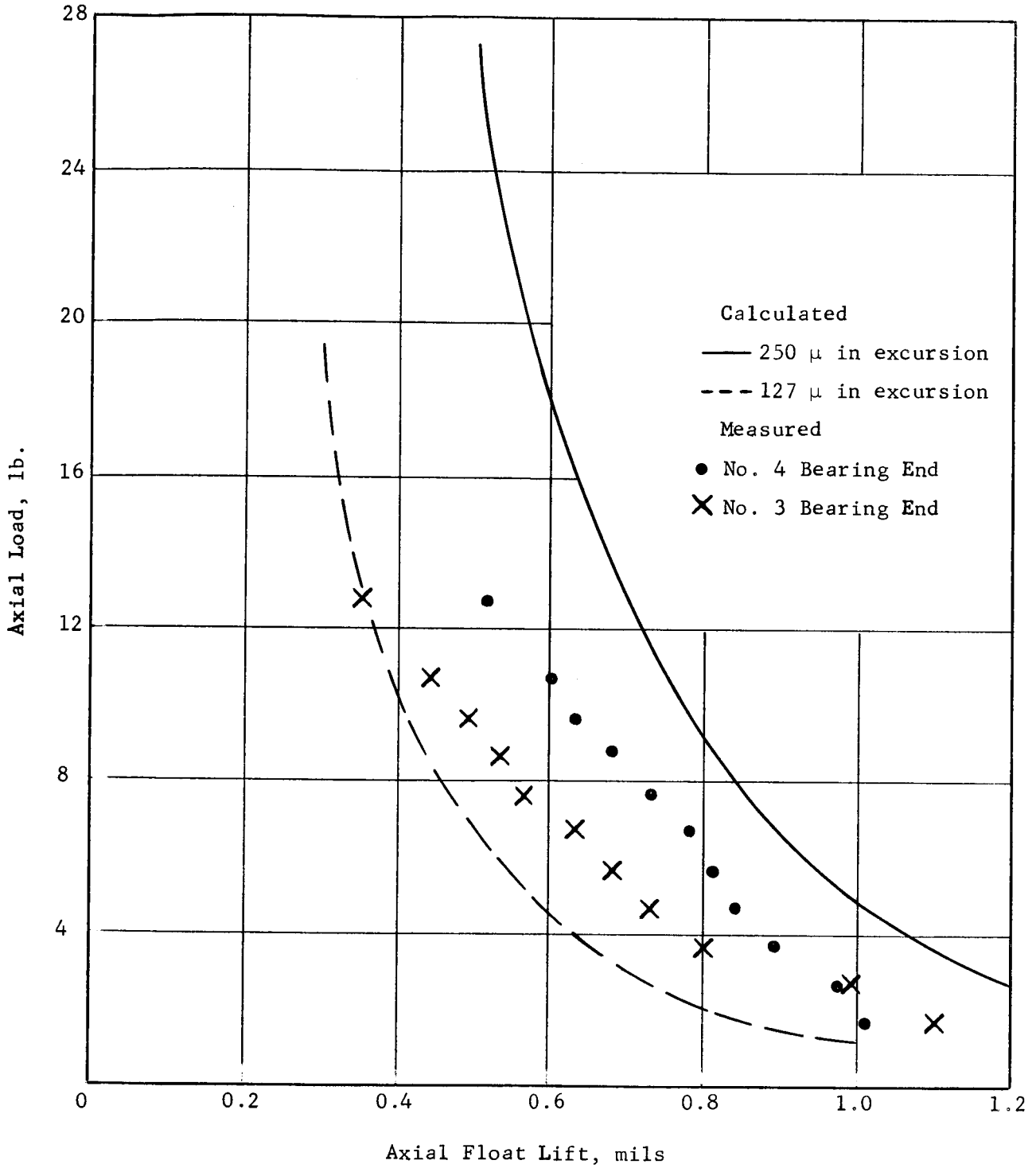

Fig. 16 Calculated and Measured Float Axial Load Capacity